



The Open Fuels & Energy Science Journal

Content list available at: www.benthamopen.com/TOEFJ/

DOI: 10.2174/1876973X01710010048



RESEARCH ARTICLE

Comparison of Two Coal-Gasifier-Designs with Moving-Bed and Internal-Circulating-Fluidized-Bed Configuration in One Reactor

Martin Schurz*, Alexander Laugwitz, Steffen Krzack and Bernd Meyer

Department of Energy Process Engineering and Chemical Engineering, TU Bergakademie Freiberg, Fuchsmühlenweg 9, Reiche Zeche, 09596 Freiberg, Germany

Received: February 08, 2017

Revised: May 19, 2017

Accepted: June 13, 2017

Abstract:

Background:

Coal gasification is the promising technology for syngas routes to produce chemicals or transportation fuels. Additionally, it enables clean power generation from coal in Integrated Gasification Combined Cycles (IGCC). So far, coal fines with high ash contents could not be feasibly used in such routes.

In this regard, the Internal Circulation gasifier (INCI) is designed to gasify high-ash coal fines efficiently. The staged system is combining a moving bed, a fluidized bed and a jetting fluidized bed in one reaction chamber.

Method:

The present paper substantially describes the laboratory-scale prototype development in the COORVED-project (“CO₂-reduction by innovative gasifier design”) based on the INCI gasification principle of about 50-125 kW thermal input. Information about the gasifiers compounding, especially the reaction chamber, peripheral components and applied measurement systems are given.

Results:

Experimental results are presented, confirming the targeted, typical flow pattern inside the reaction chamber. Furthermore technical and operational limits of the COORVED prefiguration are discussed. Based on these results a major design change of the reaction chamber is required and explained in detail. Additionally, results of the feedstock variation from coke to lignite are shown.

Conclusion:

Finally, the operability of the INCI gasification principle is proven by a stationary operating system with controlled ash agglomeration.

Keywords: Fluidized bed gasification, High-ash coal, COORVED gasifier, INCI, Internal circulation, Ash agglomeration.

1. INTRODUCTION

1.1. Concept of Internal Circulation Gasification Principle

The INCI gasifier, which was developed and patented by the TU Bergakademie Freiberg, is designed to be especially suitable for high-ash coal fines [1 - 9]. It provides the possibility to convert this difficult feedstock, which usually remains unused, into a synthesis gas. Gräbner *et al.* [10] are defining the thermodynamically optimal operation temperature for coals with different ash contents (5-45 wt.% (wf)). This optimal temperature is found between 1,200 K and 1,600 K for a 30 bar gasifier. As an example, a high-ash South African coal with an ash content of 25.3 wt.% (wf)

* Address correspondence to this author at Department of Energy Process Engineering and Chemical Engineering, TU Bergakademie Freiberg, Fuchsmühlenweg 9, Reiche Zeche, 09596 Freiberg, Germany; Tel: +49-(0)3731-39 4483; E-mail: martin.schurz@iec.tu-freiberg.de

has an optimal exit gas temperature of 1,253 K or 1,408 K for maximizing cold gas efficiency or syngas yield, respectively. Thus the targeted gas outlet temperature for the INCI gasifier concept is 1,270-1,370 K in order to approach the thermodynamically optimum for a wide range of high-ash coals. The mean operational temperature in the reactor is 50-100 K higher. This temperature is between the ash softening and fusion temperature for most coals. In this temperature range, coal particles tend to be sticky. If the volume fraction of particles is sufficiently high, agglomerates might be formed. These conditions can be found in agglomerating fluidized-bed gasifiers, such as the U-Gas gasifier [11 - 13], the AFB (or ICC CAS) gasifier [14] or the KRW gasifier [15]. These agglomerating fluidized-bed gasifiers achieve carbon conversion rates above 95%. Based on the U-Gas-technology the company Synthesis Energy Systems is currently marketing fluidized bed gasifiers with ash-agglomeration. Gräbner [3] mentioned two U-Gas-gasifiers each of 400 t/d coal currently operating in China, Zaozhuang City. Also the AFB-gasifier is currently operating in China with units up to 324 t/d coal [3]. However, a post treatment of the bottom ash and dust is still necessary in these commercial ash-agglomerating gasifiers. The INCI gasifier concept is a combination of an agglomerating fluidized-bed and a moving-bed gasifier. Combining several flow patterns inside the gasifier allows for internal post-gasification of carbon-containing agglomerates. The major drawback of fluidized bed gasifiers of restricted carbon conversion can be eliminated by the ash agglomeration. Thus, a selective separation of ash from the fluidized bed is possible, which reduces the carbon losses by the bottom product. As a result, the overall carbon conversion rate is above 99% and an external post-treatment of the bottom product is not required. Bituminous coal, lower in reactivity, can be successfully converted as well. Due to its raw gas outlet temperature (1,270-1,370 K), the INCI gasifier shows the highest cold gas efficiency and syngas yield, compared to the other investigated gasifiers, if high-ash coals are processed [10, 16]. Difficulties of ash agglomerating gasification processes, working just in a small range of feedstock specific optimal settings, can be neglected in the INCI-gasifier, due to its manifold opportunities of precise local temperature control. The increased oxygen consumption compared to non-agglomerating fluidized bed gasifiers [3] is also balanced by the high performance regarding the achievable cold-gas-efficiency and syngas-yield in the INCI-gasification-process. The simulation-based expectations on the industrial-scale INCI-plant are given by Gräbner [3], leading in high values for cold-gas-efficiency > 83.5% and syngas-yield > 1.85 m³(H₂+CO;STP)/kg(waf) at a carbon conversion above 99%. The calculation for the industrial scale unit (thermal capacity: 500 MW) is based on heat losses (heat transferred to the water-wall) of about 1.5%. The INCI gasifier is showing very good performance compared to other fluidized bed gasifiers, especially for high-ash coals.

1.2. Flow Pattern of INCI Gasification Principle

As shown in Fig. (1) and mentioned in [1 - 5], the INCI gasifier combines different flow patterns in one reaction chamber. A moving bed can be found at the bottom. Here, the post-gasification of carbon-containing agglomerates takes place using an oxygen-containing secondary gasification agent. Above the moving bed different fluidized-bed zones evolve with height. Between the moving bed and the level of coal feeding and injection of the primary gasification agent, a bubbling or turbulent fluidized bed is present. Gases, leaving the moving bed at its top, serve as fluidization agent. These gases are a mixture of syngas from post-gasification and unreacted secondary gasification agent. The temperature in this fluidized-bed zone is below the ash sintering point (T_{sinter}), thus no formation of agglomerates is possible there. For some ashes the sinter temperature can be several hundred Kelvin below the initial deformation temperature [11, 17, 18]. Because the targeted particles are coal fines, usually < 500 μm, a lower fluidization velocity is required in comparison to conventional fluidized beds.

At a certain height, the primary gasification agent is added. Several nozzles are distributed around the circumference of the vessel, providing an oxygen-steam mixture as high-velocity gas jets. Because the nozzles are positioned in a boxer arrangement, these jets will conjoin and an up-flowing central gas jet evolves. In this manner, a jetting fluidized bed, described *e.g.* in [19, 20], is established. At the same level the coal is fed. Oxygen in the central jet promotes exothermic combustion reactions. Consequently, the jet will yield a central flame-like zone, with temperatures (T_{jet}) above 2,300 K. Due to the nature of a free jet, a recirculation cell emerges. Whilst the fast up-flowing jet has a void fraction close to unity, the down flow in the annular region shows an increased particle volume fraction. The higher particle load in the recirculation cell is expected to protect the reactor wall from high flame temperatures. Moreover, the recirculation cell will increase the particle residence time in this main reaction zone. As indicated in Fig. (1), the average temperature in the recirculation cell ($T_{\text{recirc.cell}}$) is below the ash fusion temperature. However, in this jetting fluidized-bed zone particle agglomeration is expected to take place as the temperature is above T_{sinter} . Note that besides an adequate temperature, a certain degree of carbon conversion or a certain minimum for the bed ash concentration must be reached, before agglomeration can occur [11, 17, 21, 22]. The hot central jet induces considerable thermal

buoyancy. The particles from the bubbling fluidized bed below are sucked into the jetting fluidized bed zone above continuously by means of pressure differences resulting from different velocities, which ensures constant presence of fuel in the oxygen rich zone, especially in interaction with control of the expansion height of the lower fluidized bed.

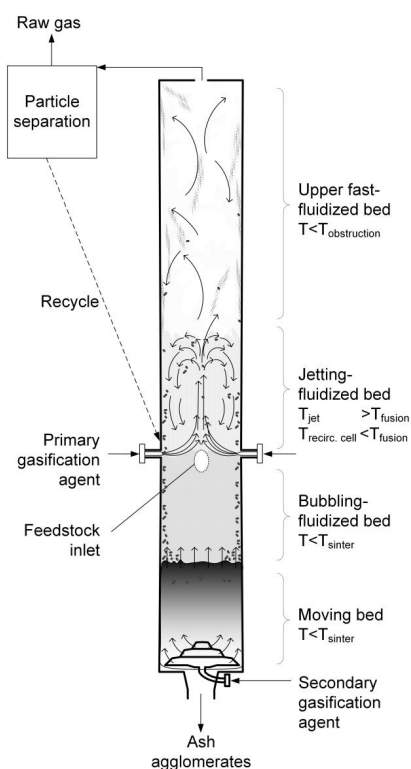


Fig. (1). Scheme of an INCI-gasifier [23] - graphic modified.

At the upper end of the main reaction zone, at the changeover to the post-gasification area, fine particles tend to form strands and clusters rather than traveling upwards isolated from each other. This increases the probability for further agglomeration of circulating and entrained fines. Moreover, the entrainment velocity of strands is increased, compared to the single particles, which reduces particle discharge at the top. No oxygen is present in this upper zone and endothermic reactions lead to a decrease of temperature to the targeted outlet temperature of approx. 1,270 – 1,370 K. In regard to reduce degradation and fouling at the surfaces of gas outlet ducts and subsequent heat exchangers, attention should be paid on keeping the outlet temperature below the obstruction temperature ($T_{\text{obstruction}}$), which is specific to a certain ash [23]. Especially the melting behavior of the fuels mineral matter under reducing atmosphere and the residual carbon content of the dust in the raw gas is having an influence on solids depositions in downstream equipment [3] and on the temperature limit in the upper fast fluidized bed. Due to agglomeration of fines in the jetting zone and the fast fluidized zone, fly ash carry over is reduced. However, it is known from fluidized bed gasification, that a certain amount of carbon containing fly ash particles can serve as surface for condensing alkali and earth alkali metals [24]. Thus, degradation and fouling of exit ducts and heat exchanger surfaces is markedly reduced. Hence, a certain amount of fly ash carry over is appreciated. If necessary, downstream particle separation (*e.g. via* candle filter) and subsequent recycle into the gasifier can be applied.

The agglomerates, generated in the hot zones, are too heavy for fluidization under the given flow conditions. They fall down and form a moving bed at the bottom of the reaction chamber. These agglomerates have a carbon content of approx. 5-20 wt.%. Secondary gasification agent is fed from below. It is a mixture of oxygen and steam or carbon dioxide. For the avoidance of hot spots in the moving-bed, the upper limit of oxygen content should be in the range of 10-15 vol.%. Thus, temperatures are kept below the ash sintering temperature to avoid clinkering and to ensure a stable flow through the bed. The flow rate of secondary gasification agent is set to meet the required fluidization velocity for the bubbling fluidized bed zone directly above the moving bed. Post-gasified agglomerates have carbon contents below 5 wt.%. They are discharged at the bottom by means of a rotary grate as applied for conventional moving-bed dry-bottom gasifiers [3].

Preliminary work, investigating the targeted conditions in the central hot reaction zone (flame zone) and the region above, which is dominated by endothermic reactions, is presented in [7]. Here an inverse diffusion flame was developed and configured to represent the condition in the INCI gasifier. Experimental investigations and numerical simulations are in accordance and show the expected overall behavior of the oxidizing hot reaction zone and endothermic reaction zone above. Additional preliminary work is designated to numerical simulation of the flow pattern inside the reaction chamber [25]. It is shown how an Euler-Euler based approach is able to predict the fluidization behaviour and particle distribution for ambient, non-reacting conditions. Both preliminary works indicate that the targeted operational principle is feasible.

2. EQUIPMENT

2.1. Laboratory-Scale INCI Coal Gasifier COORVED

The implementation of the INCI gasification principle was carried out by two different lab-scale gasifier designs. Within the framework of the COORVED project the gasifier unit was successfully started-up at TU Bergakademie Freiberg, in 2014 [6].

There are several modifications of the COORVED gasifier compared to the large-scale INCI unit, as indicated in [4].

The reactor, shown in Fig. (2), is a vertical tube reactor of about 5.5 m in height.

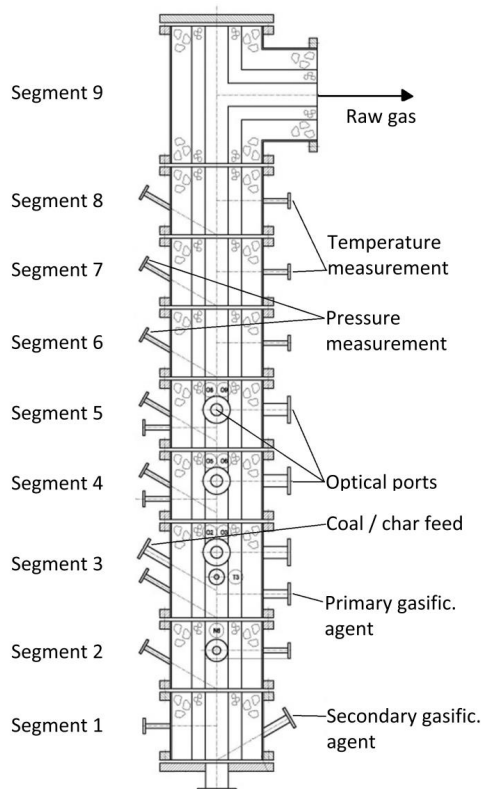


Fig. (2). Segmented construction of the COORVED reactor [4]- graphic modified.

At the bottom of the reaction chamber, a cone valve sluice is applied to discharge the moving bed. Fly ash particles are separated and collected in the raw gas filter, operating up to 823 K.

Primary gasification agent is fed through a lance in the third segment (see Fig. 2). Depending on temperature, volume flow and nozzle diameter (3-4 mm) a nozzle gas exit velocities of 30-100 m/s can be set. The superficial gas velocity, resulting from feeding of secondary gasification agent below, is crucial. It can be influenced by the mass flow and electrical pre-heating. Both gasification agents can be pre-heated up to 523 K to avoid cold zones and steam condensation.

Several reactor segments are equipped with temperature and pressure measurement tools to gain information about necessary process data and to prevent critical conditions.

After the raw gas leaves the reactor at the top, gas analysis is done by a gas phase chromatograph (GC) 3000 Micro GC (Inficon) and a Fourier-Transform-Infrared-Spectrometer (FTIR) CX-4000 FT-IR (Ansyco).

A radiometric level detection is installed at the two lower reactor segments. It is divided into two separate measurements, a vertical rod radiator (based on cesium-137) and sensor above the secondary gas inlet and a radiometric spot measurement at the upper end of segment 2 (Fig. 3).

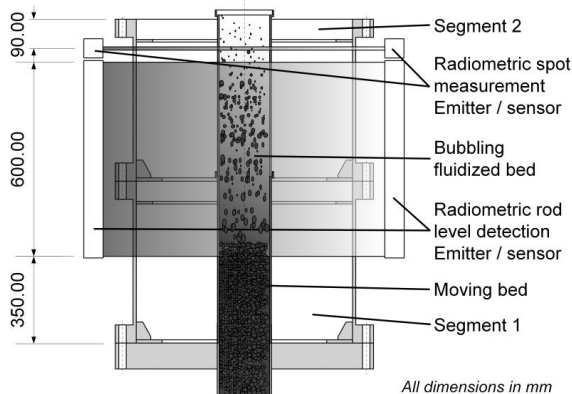


Fig. (3). Schematic arrangement of the radiometric measuring equipment.

The measurement system enables for estimation of the accumulated solids in the moving-bed and the bubbling-fluidized-bed zones of the reactor.

2.2. Reaction Chamber Design

In the present paper two steps of the prototype development of the lab-scale gasifier COORVED are compared with each other. Both are designed for 50-125 kW thermal input. The first version (V1), which was already described [4 - 6], and the second design, the reaction chamber (V2), are opposed to each other in Fig. (4).

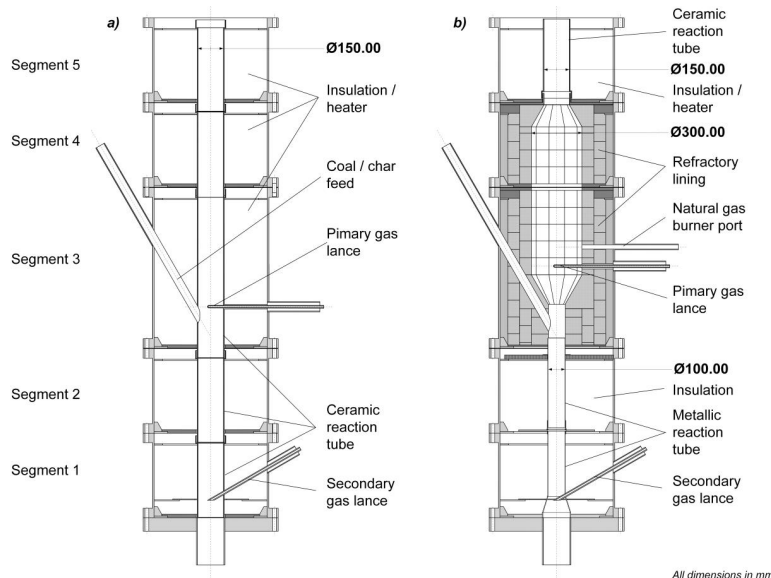


Fig. (4). Central part of COORVED reaction chamber in a) design V1 and b) the modified configuration V2.

The whole V1-reaction chamber from the bottom, where the ash agglomerate sluice is situated, to the raw gas duct on the top is of constant inner diameter. Hence, all segments, except the reactors top, are composed of a double layer

insulation of aluminosilicate mats, a vacuum molded padding, each with embedded 12 kW electrical heaters made of chrome-iron-aluminum-alloy, and a ceramic reaction tube with an inner diameter of 150 mm (Fig. 5).

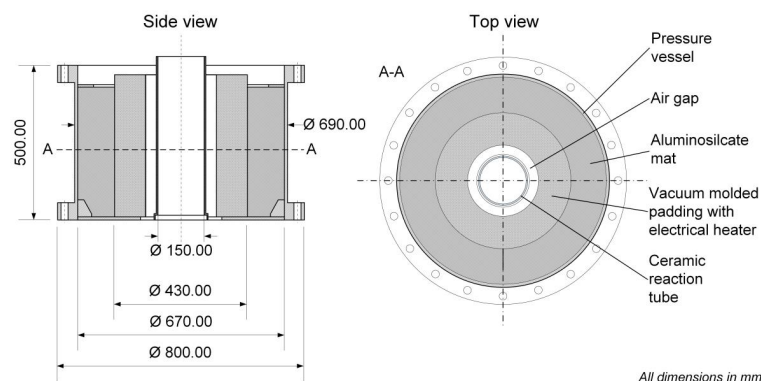


Fig. (5). Simplified scheme of a single reactor segment in V1 without measurement ports – as partially described in [4]- modified side view.

The top reactor segment differs from the segments below. It is not equipped with electrical heaters and the vacuum molded padding is replaced by several layers of aluminosilicate mats.

In the central part (segment 3 to 4) (see Fig. 4) the recirculation cell emerges and the main part of the carbon conversion is expected to take place. Thus, the third, fourth and fifth segments are each equipped with three optical ports in addition to temperature and pressure sensors. The optical ports of the reactor are prepared for particle-image-velocimetry-measurement, to visualize the flow conditions in the recirculation cell, and for optical temperature measurement, which is not installed yet in gasification operation due to transmissivity issues of the inner glasses.

Modifications of the reactor design V2 were done especially in the reaction chambers inner diameter (see Fig. 4 – b). The inner diameter of segment 1 and 2 is reduced from 150 mm to 100 mm, which reduces the minimum required secondary gas volume flow to prevent settling of unreacted feedstock particles. The inner diameter of the main reaction zone (segments 3 and 4) is widened from 150 mm to 300 mm. The connection between the reduced and the enlarged radius is done by a 60° conical widening. By increasing the cross section the superficial gas velocity in the main reaction zone is essentially decreased. Therefore, the higher distance between the reactor's inner wall and the central flame zone and the raised ratio between superficial gas velocity in the main reaction zone and primary gas nozzle outlet velocity result in improved conditions for the formation of the recirculation cell. Moreover, the risk of ash or slag deposits on the reactor's wall is expected to be lower. Furthermore, the connector between segments 4 and 5, from an inner diameter of 300 mm to 150 mm, is also realized as a cone of 60°.

In start-up-operation, the refractory lined central part of the reactor is heated up by a natural gas burner until the wall in segment 3 reaches a temperature of 1023 K. During gasification operation, segments 5 and 6 are incipiently electrical heated as heat losses are high due to the slim design.

3. EXPERIMENTAL

3.1. Feedstock Characterization

Two different feedstocks were utilized in the COORVED reactor for the present paper, a powdery hearth furnace coke made of Rhenish lignite, hereinafter simply called coke, and dried Lusatian lignite, henceforth referred as lignite. The feedstocks were specified by the framework of the COORVED project. The coke was applied both in reactor design V1 and V2, whereas the lignite was only fed in V2 as a mixture with the coke.

The powdery hearth furnace coke is produced at a pyrolysis temperature of 1,173 – 1,223 K and has an inner surface area of about 300 m²/g (BET; according to DIN 66131 and 66132 with nitrogen at 77 K). The coke is not further pre-treated. The utilization of coke, especially as the feedstock of choice for pre-heating, is reducing the risk of tar and oil deposition. Furthermore the high fusion temperature of the cokes mineral components avoids slagging operation in heat-up-phase even at high oxygen supply. Another key advantage is the high carbon content of the coke, leading to carbon-containing residues in the moving bed zone, which are especially favorable in the pre-heat-procedure of the

lower reactor section.

By reasons of its moisture content (11.4 wt.% in delivery condition) the feeding properties of the fine lignite were unfavourable. The material needs to be dried to at least 7.0-8.0 wt.% moisture content to ensure continuous input. Due to its high volatile matter and the *in-situ* production of highly reactive coke, the utilization of coal is advantageous for agglomeration-promoting conditions in the main reaction zone. The fast reaction of the volatiles and the coke with oxygen results in raised local temperatures. The increased temperature in the central flame zone is beneficial for partially melting of the fuel ash, which is necessary for the formation of agglomerates.

Both powdery feedstocks have a comparably particle size distribution (Table 1).

Table 1. Particle size distribution, heating value, bulk density, surface area for coke and lignite.

Fuel	Volume based particle distribution – Q3			Heating value in kJ/kg (wf)	Bulk density in kg/m ³
	10%	50%	90%		
	in μm				
Coke	13.8	79.3	239.9	29.8	525
Lignite	13.1	67.9	232.1	25.4	461
German DIN Standard	66165-2			51900	51705

wf: water free

According to the DIN Standard, the sample moisture (DIN 51718), proximate analysis (DIN 51718, 51719 and 51720) and ultimate analysis (DIN 51732) of both feedstocks are given in Table 2.

Table 2. Proximate and ultimate analyses of coke and lignite.

Fuel	Proximate analysis				Ultimate analysis				
	Moisture	Ash	Volatiles	C _{fix} *	C	H	N	S _c	O*
	wt. %	wt. % (wf)	wt. % (wf)	wt. % (wf)	wt. % (waf)	wt. % (waf)	wt. % (waf)	wt. % (waf)	wt. % (waf)
Coke	0.96	10.01	4.77	85.22	98.49	0.26	0.27	0.44	0.54
Lignite	11.40	5.69	52.06	42.25	69.18	4.91	0.71	0.49	24.71

wf: water free; waf: water and ash free; *: calculated by difference; c: combustible

Table 3 shows the results of the XRF ash analyses according to DIN 51729-10.

Table 3. XRF analyses of coke ash and lignite ash.

Fuel	Oxide content in wt. %										
	Na ₂ O	MgO	Al ₂ O ₃	SiO ₂	K ₂ O	CaO	TiO ₂	Fe ₂ O ₃	BaO	SO ₃	Balance
Coke ^a	3.43	17.74	4.12	0.57	1.61	31.34	0.23	12.52	0.35	16.84	11.25
Lignite ^a	d.l.	9.90	4.30	9.38	0.19	25.17	0.22	26.82	0.12	22.00	1.90

wf: water free; d.l.: below detection limit; ^a: ash 450 °C

The XRF-analyses are showing differences in the content of components influencing the ash fusion behavior. Especially the iron content, which absolute amount is almost doubled in case of lignite, is identified to play an important role in ash agglomeration [11, 22].

Table 4 summarizes the ash fusion behaviour of the mineral matter according to DIN 51730 and the additional Initial shrinking temperature, defined by Schimpke *et al.* [26].

Table 4. Ash fusion behavior of coke and lignite.

Fuel	Atmospheric conditions	Observed characteristic				
		Initial shrinking temperature	Initial deformation temperature	Softening temperature	Hemispherical temperature	Fusion temperature
		in K				
Coke ^a	Oxidizing	1,263	1,613	1,632	1,668	> 1,883
	Reducing	1103	1,544	1,584	1,650	1,764
Lignite ^a	Oxidizing	1303	1,541	1,633	1,656	1,763
	Reducing	1103	1,573	1,593	1,696	1,751

Depending on the process conditions, reducing or oxidizing atmospheres are crucial. Lignite and coke show reduced temperatures of the characteristic fusion behaviour under reducing atmosphere compared to oxidizing atmospheric conditions. The probably most important discrepancy between coke and lignite is the comparatively low fusion temperature for lignite ash in oxidizing atmosphere in contrast to the significantly higher values of the cokes mineral matter.

3.2. Experimental Design

The first course of operation in reactor design V1 focuses on the formation of the flow profile, mainly the moving bed zone and the recirculation cell as well, *e.g.* to determine the minimum secondary gas velocity, required to transport a minimum amount of solids up to the primary gas nozzle. This is necessary to feed carbon into the oxygen containing flame zone. Furthermore, a sufficient accumulation of solids in the moving bed needs to be confirmed.

The primary oxygen flow and the influence of thermal buoyancy, caused by the flame, on the formation of the circulation cell and the moving bed are examined in the second experimental series.

The last set of experiments in V1 covers the implementation of the lessons learned to increase the carbon conversion and to increase the probability of particle or ash agglomeration. Therefore, a minimum temperature is required to achieve a certain carbon conversion. On the other hand, the reactor temperature near the wall must not exceed the ash fusion temperature to avoid slagging operation.

The conditions of the targeted runs are summarized in Table 5.

Table 5. Process parameter variation of first experimental campaign in V1.

Exp. goals	Varied process parameters
Minimum secondary volume flow	Feedstock Coke Secondary gas composition N ₂ , CO ₂ /H ₂ O Secondary gas flow in m ³ /h(STP) 11.94- 22.12
Formation of recirculation cell; Temperature distribution	Feedstock Coke Primary gas composition N ₂ , CO ₂ /H ₂ O, O ₂ Primary gas flow in m ³ /h(STP) 4.5-5.4 Secondary gas composition N ₂ , CO ₂ /H ₂ O, O ₂ Secondary gas flow in m ³ /h(STP) 13.60-14.23 Stoichiometric air ratio 0.24-0.33 Total steam/O ₂ -ratio or CO ₂ /O ₂ -ratio in kg/m ³ (STP) 1.13-3.76
High carbon conversion	Feedstock Coke Primary gas composition N ₂ , CO ₂ /H ₂ O, O ₂ Primary gas flow in m ³ /h(STP) 5.4-7.0 Stoichiometric air ratio 0.33-0.42 Total steam/O ₂ -ratio or CO ₂ /O ₂ -ratio in kg/m ³ (STP) 1.53-2.56

The next campaign, having almost the same experimental goals like explained before, was carried out in reactor design V2. Due to the design changes, the development of different flow patterns inside the reaction chamber is in focus of the experimental work again (Table 6). Particularly, the formation of the moving bed, changes in the required secondary gas flow, the proof of the recirculation cell and the formation of the flow pattern in the new conical part of the main reaction zone, need to be investigated. The next step is the comparison of the two gasifier designs regarding achievable carbon conversion and ash agglomeration. Finally, a change in the feedstock has been necessary to verify the INCI gasification principle.

Table 6. Process parameter variation of second experimental campaign in V2.

Experimental goals	Varied process parameters
Minimum secondary volume flow; Formation of recirculation cell; Formation of spouted bed	Feedstock Coke Primary gas composition N ₂ , CO ₂ , O ₂ Primary gas flow in m ³ /h(STP) 6.0-11.0 Secondary gas composition N ₂ , CO ₂ , O ₂ Secondary gas flow in m ³ /h(STP) 6.00-9.00 Stoichiometric air ratio 0.27-0.39 Total steam/O ₂ -ratio or CO ₂ /O ₂ -ratio in kg/m ³ (STP) 2.64-3.30

(Table 8) *contd....*

Experimental goals	Varied process parameters
High carbon conversion; Low wall temperatures	Feedstock Coke Primary gas composition N ₂ , CO ₂ /H ₂ O, O ₂ Primary gas flow in m ³ /h(STP) 6.75-7.00 Secondary gas composition N ₂ , CO ₂ /H ₂ O, O ₂ Secondary gas flow in m ³ /h(STP) 6.75-7.50 Stoichiometric air ratio 0.39-0.46 Total steam/O ₂ -ratio or CO ₂ /O ₂ -ratio in kg/m ³ (STP) 2.88-3.14
Ash agglomeration	Feedstock Mixture coke/lignite Primary gas composition N ₂ , CO ₂ /H ₂ O, O ₂ Primary gas flow in m ³ /h(STP) 9.00 Secondary gas composition N ₂ , CO ₂ /H ₂ O, O ₂ Secondary gas flow in m ³ /h(STP) 6.75 Stoichiometric air ratio 0.42 Total steam/O ₂ -ratio or CO ₂ /O ₂ -ratio in kg/m ³ (STP) 2.49

3.3. Evaluation of Experimental Data

The gasification operation in COORVED reactor requires online monitoring. The most important parameters, like the carbon conversion X_C , the cold gas efficiency η_{CGE} and the syngas yield y_{Syn} , can be determined based on the raw gas (RG) composition and volume flow.

$$X_C = \frac{M_{C,molar} \cdot \left\{ \left[y(CO_2) + y(CO) + y(CH_4) + y(COS) \right]_{RG,wf} \cdot \dot{V}_{RG,wf} - \dot{V}_{CO_2,PGA} - \dot{V}_{CO_2,SGA} \right\}}{x(C)_{fuel} \cdot \dot{m}_{fuel} \cdot V_{molar}} \cdot 100 \% \quad (1)$$

$$\eta_{CGE} = \frac{LHV_{RG}}{LHV_{fuel}} \cdot \frac{\dot{V}_{RG,wf}}{\dot{m}_{fuel}} \cdot 100 \% \quad (2)$$

$$y_{syn} = \left[y(CO) + y(H_2) \right]_{RG,wf} \cdot \frac{\dot{V}_{RG,wf}}{\dot{m}_{fuel}} \quad (3)$$

with:

$y(n)_{RG,wf}$... Volume fraction of the gas component n in the dry raw gas,

$\dot{V}_{RG,wf}$... Volume flow of the dry raw gas,

$\dot{V}_{CO_2,PGA/SGA}$... Volume flow of carbon dioxide in primary or secondary gasification agent,

$x(C)_{fuel}$... Carbon mass fraction of the fuel,

\dot{m}_{fuel} ... Mass flow of the fuel,

$LHV_{RG/fuel}$... Lower heating value of raw gas or fuel.

4. RESULTS AND DISCUSSION

4.1. Particle Separation and Formation of Flow Pattern Below the Primary Gas Nozzle

The particle distribution in segment 2 and 3 is influenced by several parameters, *e.g.* gas velocity, viscosity, density and particle properties. A minimum gas velocity in the lower bubbling-fluidized bed is required to expand the bed up to the inlet of primary gasification agent. Because the feedstock has a certain size distribution, some particles will be transported up to the level of primary gasification agent injection, whilst others remain in the lower bubbling-bed zone or in the moving bed respectively. The calculated particle entrainment velocity, corresponding to Kunii *et al.* [27], is sufficient consistent with the experimental data of the maximum entrained particle size (see Table 7).

For high secondary gas flow rates the fine coke is carried out of the main reaction zone after inappropriate short residence time. This leads to an undesired decrease in carbon conversion in the gasification process. Another disadvantage of a high superficial gas velocity in the lower segments is the hindered formation of the recirculation cell

due to a lower shear rate between primary gas nozzle outlet velocity and the gas coming from beneath the primary gas nozzle. The risk of a blockage of the feedstock inlet by a fast increasing moving bed level is obviated even at the lower secondary gas flow rate of 14.23 m³/h(STP). The main function of the secondary gas, to carry the feedstock to the main reaction zone, needs to be preserved for safety reasons. Hence, a secondary gas flow lower than 14.23 m³/h(STP) at the given temperature is not recommended.

Table 7. Particle entrainment calculation and experimental results (823 K, coke).

Sec. gas flow rate in m ³ /h(STP)	Superficial gas velocity in Segment 2 in m/s	Entrained max. particle size - calc. acc. to Kunii <i>et al.</i> [27] in μm	Max. entrained particle size - experimental results in μm	Entrained fraction of feedstock in %
22.12	1.05	300	250	> 99
14.23	0.67	220	200	> 90

Further experiments show the influence of high oxygen contents in the primary gas. If the primary oxygen flow exceeds 2.5 m³/h(STP) the increasing flame temperature leads to improved thermal buoyancy. Consequently, the gas flow velocity beneath the primary gas nozzle increases and larger particles can be fluidized and carried from the lower bubbling fluidized bed up to the level of primary gasification agent injection. Moreover, less particles drop down onto the moving bed. The evidence of that facts have been provided by the radiometric rod and spot measurement, showing no further increase in moving bed level and bubbling fluidized bed density above 2.5 m³/h(STP) oxygen and even slightly decreasing values for higher oxygen flow rates (Fig. 6). The radiometric measurement delivers an integral value of the moving-bed height and/or the bubbling-fluidized-bed density, in which 100% equates a fixed bed over the whole measured area.

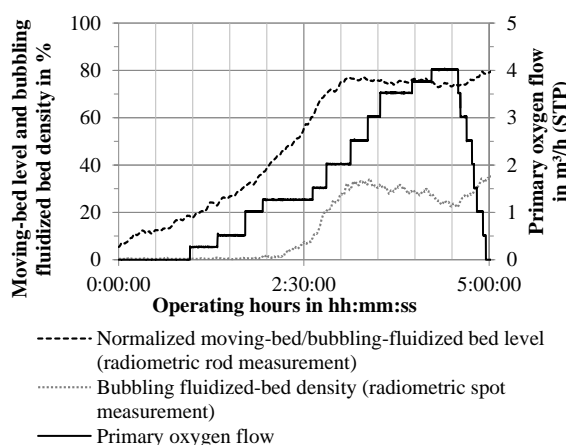


Fig. (6). Influence of oxygen content in primary gas on relative change of bed density and bed level in reactor design V1.

Based on the findings of the oxygen addition further experiments can be conducted with lower secondary gas flows if the primary oxygen flow exceeds 2.5 m³/h(STP). The gas flow rate of 13.60 m³/h(STP), leading in a superficial gas velocity of 0.64 m/s in segment 2, has been identified to be the lower limit of the secondary gas flow rate for gasification operation. As mentioned before, in the gasification process a sufficient low superficial gas velocity is beneficial.

In reaction chamber design V2 the secondary gas volume flow can be reduced to the range of 6.00-9.00 m³/h(STP) through the changes in the lower reactor section. Consequently, the resulting superficial gas velocity amounts to 0.88-1.16 m/s in the upper segment 2 or lower segment 3 respectively. Reasons for the raise in superficial gas velocity, compared to V1, are depending on the evolving flow pattern in the lower main reaction zone, the conical part, of V2. The ratio of 1:3 between the reaction tube diameter in the lower part (segment 1 and 2) and the main reaction zone diameter (segment 3 and 4), the angle of the conical widening and the set gas velocities combined with the powdery feedstock are causing the formation of a spouted bed, as described by Duarte *et al.* [28]. The bed consists of an annular moving-bed and a fast fluidized central flow with recurrent particle throw-offs. The necessary fast base fluidization requires higher superficial gas velocities below the conical widening. The formed spouted bed has advantages for the

gasification process, first of all for the accumulation of carbon-containing solids in the lower main reaction zone. The particle buildup and the evolving spouts into the flame zone are beneficial for the conversion process and ash agglomeration.

4.2. Comparison of the Local Fluid-Bed Status in Designs V1 and V2

To exemplify the general flow pattern in gasification for both reactor designs the REH-diagram [29] is used (Fig. 7). It shows the operation in V1 and V2 result in similar flow conditions, both corresponding to INCI-gasification principle.

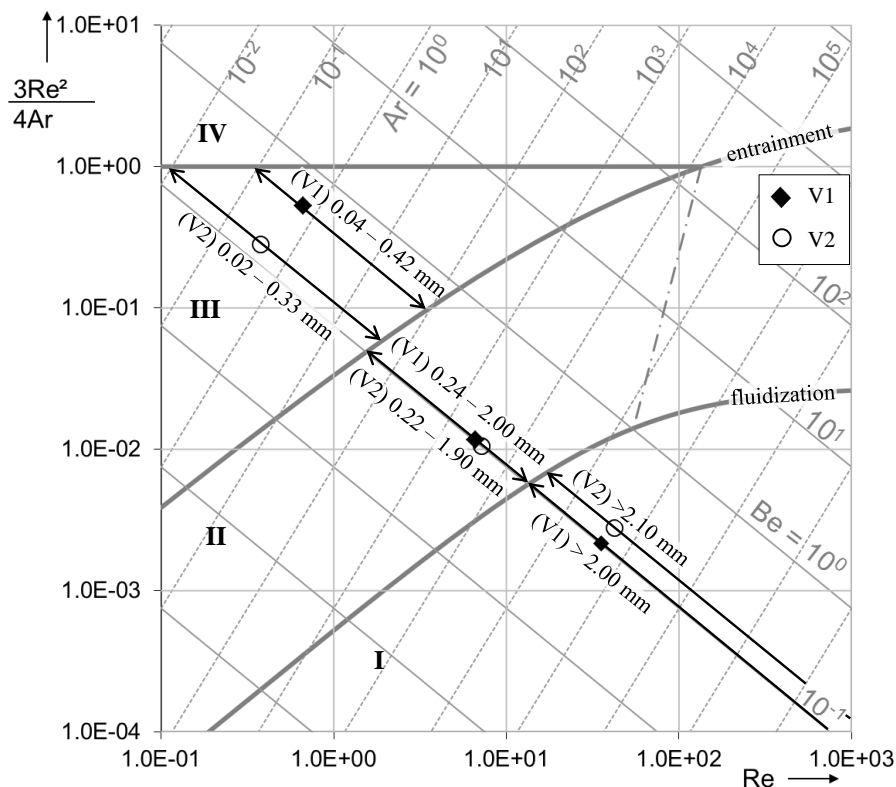


Fig. (7). REH-diagram of flow pattern in exemplary gasification operation for V1 and V2.

The required settings for the illustration in REH-diagram are given in Table 8, where D_{ret} Specifies the inner reaction tube diameter and T is the average temperature in the respective reactor zone. Both values are influencing the specific superficial gas velocity v_{gas} which is crucial for the evaluation of the fluid status for particles of a defined Sauter diameter $d_{p,S}$.

Table 8. Operating conditions of gasification in V1 and V2 for REH-Diagram.

Reactor design	Reactor zone	Area in REH-diagram	D_{ret} in mm	T in K	v_{gas} in m/s	$d_{p,S}$ in mm
V1	Fixed bed	I	150	790	0.64	5.0
	Bubbling fluidized bed	II	150	849	0.69	1.0
	Jetting Fluidized Bed	-	150	1579	2.0	0.079
	Upper post-gasification zone	III	150	1189	1.52	0.079
V2	Fixed bed	I	100	861	0.75	5.0
	Bubbling fluidized bed	II	100	773	0.68	1.0
	Jetting Fluidized Bed	-	300	1428	0.3	0.068
	Upper post-gasification zone	III	150	1215	1.05	0.068

Area I in REH-diagram, below the minimum fluidization line, is showing the fixed bed or moving bed conditions. At the given flow conditions the ash agglomerate of the average size of 5.0 mm stays in fixed bed. Particles with a

diameter below 2.0 mm (V1), or 2.1 mm (V2) respectively, are fluidized and can be found in the bubbling fluidized bed zone above (area II in REH-diagram between the minimum fluidization line and the entrainment line), which is consistent with the experimental findings, showing pre-agglomerates < 2.0 mm and oversize grain of the feedstock in that zone. Particles of the diameter less than 0.24 mm (V1) or 0.22 mm (V2) are entrained into the main reaction zone, which can be reflected in the experimental findings, too, showing the fluidization of the bigger part of the feedstock (according to Table 7).

The following main reaction zone, the jetting fluidized bed zone, can't possibly be illustrated in the REH-diagram due to its complex flow pattern, especially the recirculation cell, and the high gradients in temperature and gas composition.

The post gasification zone above (upper fast-fluidized bed) shows significant flow differences in comparison of both reactor designs. The superficial gas velocity in V1 results in single particle entrainment below 0.42 mm in diameter and for particles less than 0.33 mm in V2. In both designs particles of the average diameter cannot be entrained when they are forming particle strands, but V1 is operating closer to area IV in REH-diagram, and thereby closer to particle strand entrainment. In design V1 particles below 0.04 mm in diameter are entrained even in strands, while V2 shows entrainment only for particle strands with a grain size < 0.02 mm. Reasons for the differences in flow pattern of V1 and V2 in area III of the REH-diagram are based on the overall lower gasification agent supply in V2, resulting in a significant lower superficial gas velocity in the upper post gasification zone (see Table 8). Additionally, it needs to be considered, that because of the widened diameter of the reaction tube in V2 the superficial gas velocity in the main reaction zone is much lower than inside the entry to the tightened post gasification zone, whereby just smaller particles can enter the upper reactor part. Experimental results confirm that conclusion, since filter dust contains about 90% of particles below 0.1 mm. In geometry V1 this beneficial step in superficial gas velocity is missing and thus the major part of the residual solids reaching the upper main reaction zone is entrained. However, the overall amount of filter dust exiting the reactor by raw gas is reduced in V2 by ash agglomeration and by the shown advantageous flow pattern in the central and upper reaction tube.

4.3. Formation of the Circulation Cell

Due to the very low inner diameter of the lab-scale gasifier, the formation of a sufficient large recirculation cell needs to be confirmed, especially for the slim design V1. Therefore, Schimpke *et al.* [4] investigated the flow patterns above the primary gasification agent nozzle in a cold gas test facility of COORVED reactor geometry V1. The experimental results show good accordance with CFD-simulations of Laugwitz *et al.* [5]. Besides the investigation of the flow pattern in a cold system or CFD simulations a hot reactive system needs to be demonstrated.

In consequence of the difficulties in the transparency of the optical ports in gasification operation the determination of the formation of the recirculation cell is done by temperature measurement in the central zone. Therefore, the dependency on the settings of the primary gas composition, especially its volume fraction of oxygen, needs to be examined. The oxygen content is increased stepwise by replacing the same amount of nitrogen in the primary gas (see Fig. 8). Thus, the total primary gas volume flow and consequently the gas velocity exiting the nozzle can be kept constant up to 3.25 m³/h(STP) of oxygen in the primary gas for design V1. The primary gas mixture includes at least 0.5 m³/h(STP) of carbon dioxide. *via* the displayed temperature distribution the exact dimension of the recirculation cell is not allocable, but recycled hot gas of the flame zone is detectable. Thus, the temperatures can indicate the formation of a recirculation cell around the flame zone. But the evidence of the recirculation in the hot reactive system needs to be produce by optical measurements later on, as it was done by Schimpke *et al.* [4] in the cold test facility before.

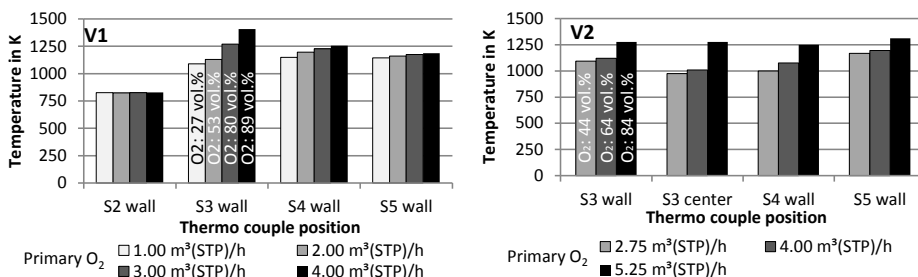


Fig. (8). Formation of the recirculation cell around the flame zone in reactor design V1 and V2 in coke gasification depending on the primary gas oxygen flow and concentration.

Even though, the primary gasification agent is actually injected into segment 3, Fig. 8 - V1 shows that the reaction tube temperature in segment 4 is as sensitive to the oxygen content in the primary gas as in segment 3 up to an oxygen flow of 2.0 m³/h(STP), which equates to about 53 vol.% oxygen in the primary gas. This effect occurs similarly for experiments using steam or carbon dioxide, respectively. It arises from the positioning of the thermocouples in the reaction tube close to the wall (see Fig. 9). Generally, an increase in oxygen addition results in a higher central flame temperature and thus intensifies the recirculation. For oxygen flows less than 2.0 m³/h(STP), the recirculation cell is comparably small and is not extended to the reactor's inner wall. Thus, the region close to the reactor's wall is not heated up by hot, recycled reaction gases but moderated by the cooler secondary gas coming from beneath (see Fig. 9-a).

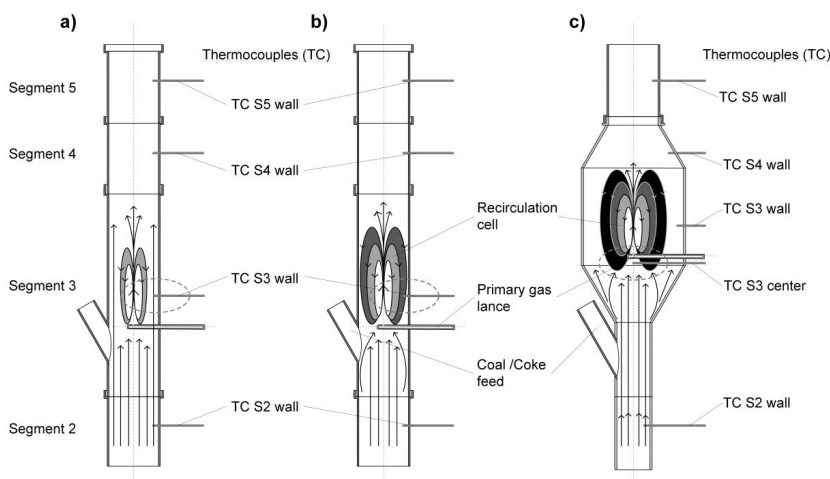


Fig. (9). Scheme of recirculation influence on temperature in segment 3 and 4 in reactor design V1 for **a)** low oxygen, **b)** high oxygen supply and **c)** in design V2 for high oxygen supply.

As a consequence, thermocouple TC S3 does not react to increased central temperatures as much as thermocouple TC S4. In the investigated range, the maximum height of the recirculation cell is sufficiently below the position of thermocouple TC S4. Thus, the temperature measurement in segment 4 is not effected by the intensification and enlargement of the recirculation cell from a fluid mechanical point of view. Only the increase in mean operation temperature due to an increase in oxygen supply is measured by thermocouple TC S4. At primary oxygen flows above 2.0 m³/h(STP), starting at 55 vol.% of oxygen, the temperature rise in segment 3 is much larger than before. It can be argued, that the recirculation cell is extended over the whole tube diameter (Fig. 9-b). Therefore, hot reaction gases are transported to the wall, which results in a strong increase in temperature measured by thermocouple TC S3. In contrast, the temperature measurement above, e.g. thermocouple TC S4, shows an almost linear increase with oxygen supply for the investigated flow range, even above 2.0 m³/h(STP). Thus, mean temperatures in segment 4, 5 and higher are not affected by the size of the recirculation cell in the investigated range.

In Fig. (8) - V2 a minor effect of the primary oxygen flow on the reactor's wall temperatures in reactor design V2 can be observed. It should be noted, that the overall primary gas volume flow is about 67% higher for experiments in V2 than for V1. Up to a primary oxygen flow of 4.0 m³/h(STP) or about 64 vol.% oxygen, showing intense influence in reactor design V1, significantly implication cannot be seen in V2. Results are based on the simple fact, that the thermocouples distance to the flame zone is doubled in V2 (see Fig. 9 - c). With increasing oxygen flows within the considered range there is still no substantial rise in temperature at the walls in segment 3 and 4. For this reason an additional temperature measurement (TC S3 center) needed to be installed. It is positioned 50 mm below the primary gas nozzle on the exact central axis of the reaction tube. Even though it is situated quite underneath the primary gas inlet an appreciable influence on the temperature by further increased oxygen addition is existent (starting from 4.75 m³/h(STP) or about 76 vol.% oxygen). A simple effect of the flames radiation can be excluded due to the fact that the thermocouple is located right in the shade of the primary gas nozzle and additionally surrounded by gas with a high solid load due to the spouted bed beneath. The further rise in temperature from the wall of segments 4 to segment 5, compared to segment 3, for all oxygen settings is based on the blending of the comparatively cold flow at the reactor's wall and the hot central flow resulting from the flame in the conical constriction below thermocouple S5 wall.

Additionally the thermocouples TC 4 and TC 5 are positioned closer to the reactors central axis than TC 3 due to the reaction tubes lower inner diameter in both upper segments. In V2 the higher temperature of the wall in segment 5 compared to V1 at the highest settings of oxygen is the result of an increased total air ratio for the experiment in V2.

An advantageous finding is the overall lower wall temperature near the flame zone in design V2, without the formation of a hot spot at the wall close to the position of the primary oxygen inlet. Thus, the reactor design V2 allows for experiments with higher total stoichiometric air ratios compared to design V1.

4.4. Coke Gasification Experiments

With the results of the preliminary investigations and the gained process understanding, the first gasification runs with the experimental aim of high carbon conversion can be realized in design V1. Constant settings have been defined, such as a secondary gas volume flow of 13.60 m³/h(STP), pre-heated to 493 K, and the pre-heating of reactor segment 2 to 823 K, to ensure the major part of the solids mass flow of 10 kg/h enters the main reaction zone. Within the first gasification runs the minimum amount of 0.5 m³/h(STP) oxygen in the secondary gas, combined with a certain minimum of oxygen in the primary gas, is identified to allow for totally autothermal operation. Not only the oxidization is providing the necessary heat in the lower two reactor segments, but also the heat transfer from the main reaction zone *via* the bubbling fluidized bed.

To gain a sufficient high carbon conversion in the overall gasification process, the primary gas composition and total amount need to be varied and optimized. Most important influence seems to have the oxygen flow rate, which is directly connected to the average temperature in the main reaction zone. Limiting facts in reaction chamber design V1 are the wall temperature in segment 3, which used to be the highest measured temperature and characterizes the risk of slagging operation, next to the primary gas velocity at the nozzles exit. A highly accelerated gas jet is advantageous for the formation of the recirculation cell, but due to growing disruptive forces with increasing gas velocity it is unfavorable for the formation of ash agglomerates. Based on the coke ash softening temperatures (according to Table 4) the maximum permitted wall temperature has been set to 1,573 K. Consequently, the maximum amount for the primary gas oxygen flow, until the wall temperature limit is reached, can be defined as 4.9 m³/h(STP) ($\lambda=0.32$ incl. secondary oxygen of 0.5 m³/h(STP)) for the gasification of 10 kg/h coke in the reactor design V1 (Table 9 –A-1). This adjustment goes along with a carbon conversion of only 63.5%, which is, due to the resulting insufficient ash concentration in the main reaction zone, not enough to gain ash agglomerates. Moreover, there is still some slightly ash caking visible at the very hot parts of the ceramic reaction tube. Probably, the thermocouple position in segment 3 does not exactly hit the point of highest temperature. The risk of slagging is preventing from further oxygen addition in the primary gas. Thus, to get better experimental results it is necessary to reduce the wall temperature significantly, while the carbon conversion is increased. Additional settings are changed, such as lowering the pre-heating temperature of the secondary gas flow by 48 K and replacement of the inert gas content in secondary gas by additional temperature moderating gas components (Table 9 – A-2).

Table 9. Coke-gasification (10 kg/h in V1): Operational settings, results and temperatures in segments 3–5.

Exp.	Settings			Results	Wall Temperature in K
	Primary gas flow in m ³ /h(STP); Preheat-temp. in K	Secondary gas flow in m ³ /h(STP); Preheat-temp. in K	Total air ratio λ ; CO ₂ /O ₂ or H ₂ O/O ₂ -ratio in kg/m ³ (STP)	Carbon conversion X_C in %; Cold gas efficiency η_{CGE} in %; Syngas yield y_{SG} in m ³ /kg(STP)	
A-1	O ₂ : 4.9 H ₂ O: 0.5 Temp.: 500	O ₂ : 0.5 H ₂ O: 7.1 N ₂ : 6.0 Temp.: 493	λ : 0.32 Mod./O ₂ : 1.18	X_C 63.5 η_{CGE} 40.5 y_{SG} 1.05	S3: 1,570 S4: 1,308 S5: 1,180
A-2	O ₂ : 5.5 H ₂ O: 0.6 Temp.: 496	O ₂ : 1.0 H ₂ O: 7.1 CO ₂ : 6.0 Temp.: 445	λ : 0.39 Mod./O ₂ : 2.76	X_C 84.8 η_{CGE} 52.7 y_{SG} 1.34	S3: 1,383 S4: 1,298 S5: 1,196

The further temperature moderating gas addition (moderator) into the secondary gas in experiment A-2 needs to be done with carbon dioxide, due to technical limitations of steam supply. The mentioned changes result in a temperature drop in segment 3 of about 187 K. Approximately one quarter of the temperature decrease can be attributed to the

reduced pre-heating. The lowered heat input in segment 3 allows for raise in the oxygen flow without exceeding the defined temperature maximum of 1,573 K. Thus, in the second step the overall oxygen flow was elevated by 1.1 m³/h(STP) to 6.5 m³/h(STP) ($\lambda=0.39$). A carbon conversion of 84.8% was achieved. Nonetheless, agglomeration was not observed. The low cold gas efficiency is the result of high heat losses of about 20-25% of the total thermal input, caused by the laboratory-scale unit.

The raw gas composition of both experiments (Table 10) is showing a comparatively high carbon dioxide content in exp. A-2, which is caused by the additional added moderator.

Table 10. Product gas composition (water and purge gas free) of exp. A-1 and A-2 (coke- gasification in V1).

Exp.	Gas component	CO	CO ₂	H ₂	CH ₄	Hydrocarbons C ₂ -C ₄	H ₂ S
A-1	Volume fraction	44.6	27.5	27.8	<0.1	d.l.	d.l.
A-2	in % (wf, pgf)	41.6	41.3	17.0	<0.1	d.l.	d.l.

wf: water free pgf: purge gas free (Nitrogen free) d.l.: below detection limit

In summary, the carbon conversion using reactor design V1 is obviously not high enough to allow for agglomeration of the processes solid residues. One reason is the remaining high average carbon content in the fluidized bed of about 60 wt.%, based on an assumed inert ash content at a carbon conversion of about 85%. As can be seen from other fluidized bed reactors, an agglomeration (and defluidization) not occurs until the carbon content reaches a sufficient low value. The required minimum bed ash content is 65 wt.% [22] up to 70 wt.% [11], dependent on coal rank.

Due to the fact, that a higher operation temperature is not feasible, the particle residence time in the hot main reaction zone needs to be increased to gain higher bed ash contents. The particle entrainment cannot easily be changed by switching operating parameters, due to the reactors optimal flow conditions. This implies that the equipment's inner diameter needs to be changed, as it is realized in reaction chamber design V2.

With the modifications of V2 the maximum measured wall temperature is reduced by 150-300 K for gasification experiments with similar stoichiometric air ratios to that in V1 (see Fig. 10 – a). This conclusion is valid for the coke gasification in carbon dioxide-oxygen-atmospheres and steam-oxygen-atmospheres. Based on that result, a higher total air ratio is attainable without exceeding limiting wall temperatures. Due to the increased primary oxygen addition into the primary gas the achievable carbon conversion, even at comparatively low wall temperatures, is higher than in design V1 (Fig. 10 – b). Therefore, most of the assumed advantages of design V2 compared to V1 are demonstrated, already. It should be noted, that the results presented in Fig. (10) are merely valid for a qualitative comparison of point clouds, due to the wide range of experimental settings (see Table 5 and Table 6).

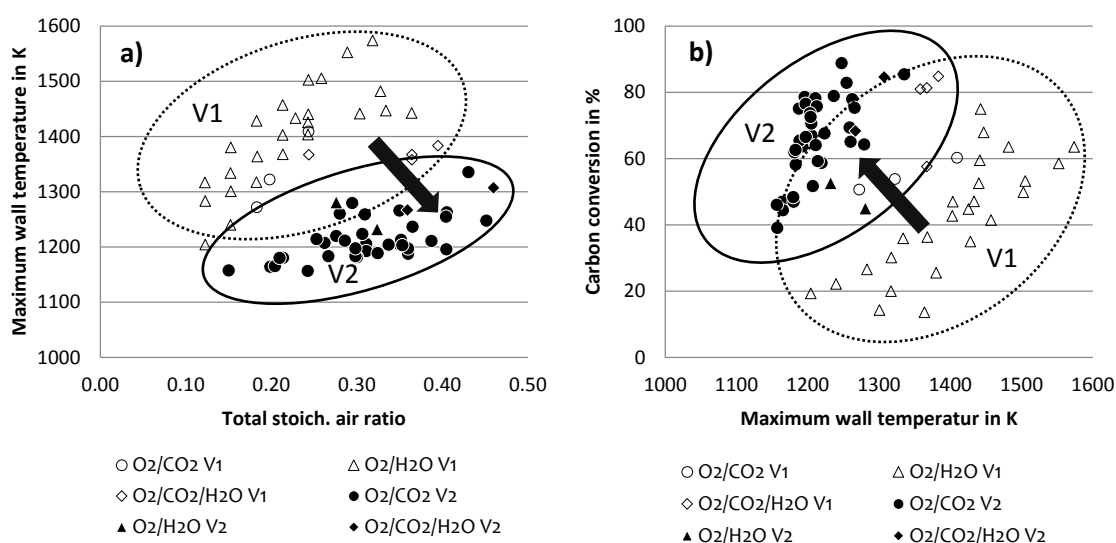


Fig. (10). Comparison of reactor design V1 and V2: a) maximum measured wall temperature depending on the total air ratio, b)

carbon conversion depending on the maximum measured wall temperature.

Variations of the solids mass flow are showing a tendency for the final gasification progress depending on the thermal input. The results of the mass flow variation indicate that the optimum for reactor design V2 is sufficient below 10 kg/h for the coke gasification (Fig. 11).

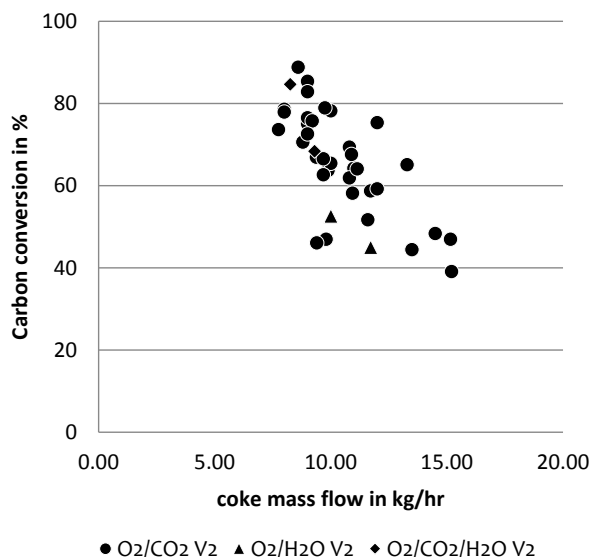


Fig. (11). Dependence of the carbon conversion on the thermal input in reactor design V2.

Due to the expected decrease in carbon conversion, caused by the cool down of the upper post gasification zone based on the higher specific heat losses at lower thermal capacity in autothermal operation, a lower limit of the solids mass flow can be assumed, too.

The reactor design V2 shows technological advance, especially due to the higher accumulated amount of solids in the main reactions zone. The inertia of the gasifier is increased compared to reaction chamber design V1. The maximum carbon conversion, which is reached in coke gasification in the reactor design V2 (See Table 11) in a mixture of carbon dioxide, steam and oxygen, is in the same magnitude as in design V1 (see Table 9).

Table 11. Coke-gasification (8.3 kg/h in V2): Operational settings, results and temperatures in segments 3–5.

Exp.	Settings			Results	
	Primary gas flow in m ³ /h (STP); Preheat-temp. in K	Secondary gas flow in m ³ /h (STP); Preheat-temp. in K	Total air ratio; CO ₂ /O ₂ or H ₂ O/O ₂ -ratio in kg/m ³ (STP)	Carbon conversion X _c in %; Cold gas efficiency η _{CGE} in %; Syngas yield y _{SG} in m ³ /kg(STP)	Wall Temperature in K
B-1	O ₂ : 5.25 H ₂ O: 1.25 CO ₂ : 1.25 Temp.: 473	O ₂ : 1.00 H ₂ O: 2.45 CO ₂ : 2.49 N ₂ : 1.01 Temp.: 493	λ: 0.46 Mod./O ₂ : 1.66	X _c 84.6 η _{CGE} 54.6 y _{SG} 1.37	S3: 1,307 S4: 1,221 S5: 1,271

Due to the lower necessary secondary gas volume flow, the raw gas composition of the experiment B-1 (Table 12) shows a higher carbon monoxide content in the water and nitrogen free gas, compared to the experiments A-1 and A-2 in reactor design V1.

Even though the amount of solids in the main reaction zone is increased and the ash content in the fluidized bed is about 65 wt.% (based on assumed inert ash content), no ash agglomeration occurs in experiment B-1. Reason can be assumed in the gasification behavior of the coke. Due to its low reactivity the partial oxidation of the coke is not

concentrated to a very small reaction volume, but extended to a larger reaction zone. Consequently the temperature has a lower local maximum and ash agglomeration is unlikely for the investigated coke gasification.

A change in feedstock to *in-situ* produced coke *via* lignite utilization is a solution.

Table 12. Product gas composition of exp. B-1 (coke- gasification in V2; water and purge gas free).

Gas component	CO	CO ₂	H ₂	CH ₄	Hydrocarbons C ₂ -C ₄	H ₂ S
Volume fraction in % (wf, pgf)	53.5	33.1	13.3	< 0.1	d.l.	d.l.

wf: water free pgf: purge gas free (Nitrogen free) d.l.: below detection limit

4.5. Lignite-Coke-Mixture Gasification

The change in feedstock to *in-situ* produced coke *via* lignite utilization is a solution for the limitation by low coke reactivity. To reduce the influence of tar formation, the feedstock is a half-half-mixture of the hearth furnace coke and Lusatian lignite.

Moisture evaporation and devolatilization of that mixture require an increase in secondary oxygen flow to provide the necessary heat especially in segments 1 and 2. The feedstock mass flow is increased to 11.5 kg/h to ensure a comparably thermal input to the coke experiments. To avoid slagging of the new feedstock, a quite high primary carbon dioxide flow is necessary to keep the temperature in the main reaction zone sufficient low. The spouted-bed temperature is relatively high due to the oxidization of volatiles in the lower segment 3. In Table 13 – C1 settings and results of the coal-coke-mixture operation are summarized.

Table 13. Coke-coal-mixture-gasification (11.5 kg/h in V2): Operational settings, results and temperatures in segments 3–5.

Exp.	Settings			Results	Wall Temperature in K
	Primary gas flow in m ³ /h (STP); Preheat-temp. in K	Secondary gas flow in m ³ /h (STP); Preheat-temp. in K	Total air ratio; CO ₂ /O ₂ or H ₂ O/O ₂ -ratio in kg/m ³ (STP)	Carbon conversion X _c in %; Cold gas efficiency η _{CGE} in %; Syngas yield y _{SG} in m ³ /kg(STP)	
C-1	O ₂ : 5.00 CO ₂ : 4.00 Temp.: 498	O ₂ : 1.75 CO ₂ : 4.49 N ₂ : 0.50 Temp.: 470	λ: 0.41 Mod./O ₂ : 2.49	X _c 84.5 η _{CGE} 50.1 y _{SG} 1.08	S3: 1,362 S4: 1,301 S5: 1,384

Experiment C-1 shows a carbon conversion of the same magnitude like in experiments A-12 and B-1 at moderate wall temperature in the main reaction zone. The comparatively low values of syngas-yield and cold-gas-efficiency are affected by the high heat losses of the laboratory-scale equipment.

The product gas composition of experiment C-1 (see Table 14) is indicating comparatively high carbon dioxide content, as it is coming along with the addition of carbon dioxide being the only moderator and again by reasons of the small scale gasifiers with its high specific heat losses.

Table 14. Product gas composition of exp. C-1 (coke-coal-mixture-gasification in V2; water and purge gas free).

Gas component	CO	CO ₂	H ₂	CH ₄	Hydrocarbons C ₂ -C ₄	H ₂ S
Volume fraction in % (wf, pgf)	51.7	43.0	5.2	< 0.1	d.l.	d.l.

wf: water free pgf: purge gas free (Nitrogen free) d.l.: below detection limit

No tars or oils in the product gas have been recognized. Thus, higher hydrocarbons, produced *via* low temperature pyrolysis, are destroyed in the hot main reaction zone by crossing the flame. Affirmatively, the gas chromatography detects no higher hydrocarbons at the product gas exit, even for the early start-up procedure with comparatively low temperature. The turbulence, caused by the jet and recirculation cell around the primary gas nozzle, is therefore expected to be very beneficial for the system.

The major drawbacks imposed by pure coke as feedstock have been solved. With the use of lignite-coke-mixture and all combined beneficial influences on the process, the ash agglomeration occurred. The agglomerates are showing a

wide range in size, from very small conglomerates of the size of the largest feedstock particles up to approx. 10 mm (Fig. 12). They can be found in the bottom product, mixed with bigger coke particles from the start-up procedure.

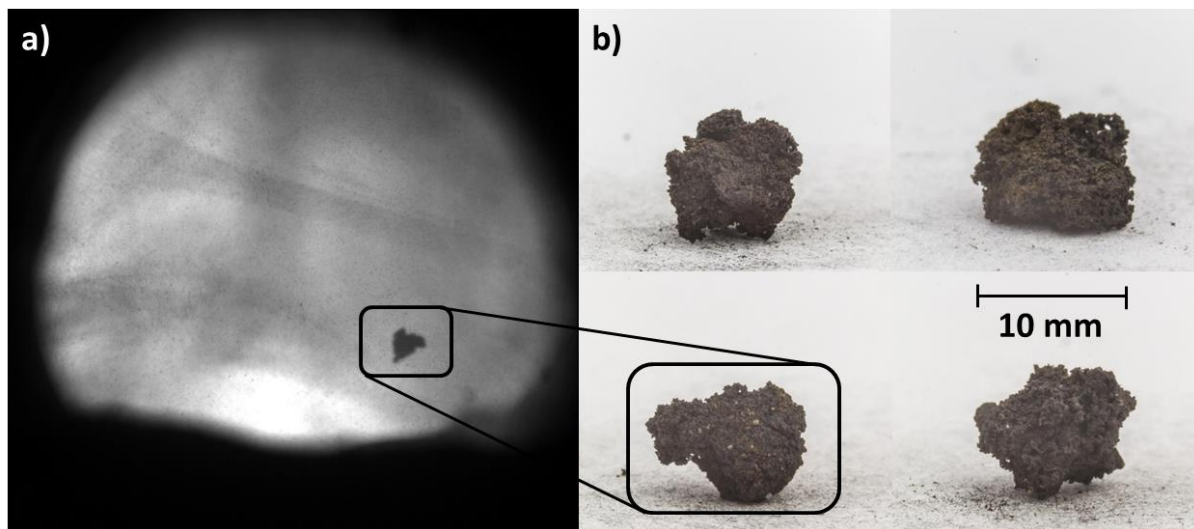


Fig. (12). Agglomerates of lignite-coke-gasification in reactor design V2: **a)** photography of falling agglomerate *via* optical excess in process, **b)** screened agglomerates from bottom product.

The results of the ultimate analysis of the agglomerates (see Table 15) confirm the expected very low carbon content.

Table 15. Ultimate analysis of ash agglomerates (coke-coal-mixture-gasification in V2).

Element	C	H	N	S _t
Content in wt.% (waf)	0.25 – 1.50	< 0.07	< 0.09	0.2 – 4.0

waf: water and ash free

CONCLUSION

The laboratory-scale internal circulation gasifier COORVED has been successfully started-up. The fundamental functionality of the flow pattern such as the formation of recirculation cells in the jetting-fluidized bed and the emergence of the moving bed in the lower reactor segments are proven. The possibility to control the temperature in the crucial segments of the reaction chamber, by different parameters, like addition of oxygen and moderators, as well as gas pre-heating temperature, is determined. As a result of further equipment optimization the reactors inner wall temperature could be reduced. The residence time of the particles in the process, by using lower gas amounts, could be increased, too. Low-reactive coke turned out to be inappropriate for ash agglomeration under the investigated conditions even in the improved reactor design. Finally, usage of lignite and consequently *in-situ* coke production in the improved reactor geometry yield better results. The ash agglomeration was confirmed and the gasifiers bottom ash has an average carbon content below 1.0 wt.%. The raw gas in lignite utilization is free of higher hydrocarbons.

ETHICS APPROVAL AND CONSENT TO PARTICIPATE

Not applicable.

CONSENT FOR PUBLICATION

Not applicable.

CONFLICT OF INTEREST

The author (editor) declares no conflict of interest, financial or otherwise.

ACKNOWLEDGEMENT

The authors appreciatively acknowledge the financial funding of the German Federal Ministry of Economic Affairs

and Energy as well as the co-funding provided by the Poerner Group in the framework of the COORVED project (R&D number: 0327865). Special thanks are regarded to K. Uebel and D. Vogt for numerous productive discussions.

REFERENCES

- [1] Gräbner, M.; Uebel, K.; Messig, D.; Meyer, B. Development and modelling of 3rd generation gasifiers for low-rank and high-ash coals, Paper 18-1, international conference on coal science and technology 26.-28.10.2009, Cape Town, ZA.
- [2] Gräbner, M.; Laugwitz, A.; Meyer, B. Development and modelling of 3rd generation gasification concepts for low grade coals, Paper # 06-1, international conference on IGCC & Xtl technologies, 3.-5.5.2010, Dresden, Germany.
- [3] Gräbner, M. *Industrial Coal Gasification Technologies Covering Baseline and High-Ash Coal*; Wiley-VCH: Weinheim, **2015**.
- [4] Schimpke, R.; Laugwitz, A.; Schurz, M.; Krzack, S.; Meyer, B. Flow pattern evaluation of the internal circulation gasification principle. *Fuel*, **2015**, *147*, 221-229.
[http://dx.doi.org/10.1016/j.fuel.2014.12.039]
- [5] Laugwitz, A.; Schurz, M.; Meyer, B. Modeling and experimental investigation of an internally circulating gasifier for high ash coals. *Pittsburgh Coal Conference*, **2014**. Pittsburgh, USA
- [6] Schurz, M.; Laugwitz, A.; Krzack, S.; Meyer, B. Start-up of internal circulation gasifier COORVED. *6th International Conference on IGCC & Xtl Technologies*, **2014**. Dresden, Germany
- [7] Stelzner, B.; Hunger, F.; Laugwitz, A.; Gräbner, M.; Voss, S.; Uebel, K.; Schurz, M.; Schimpke, R.; Weise, S.; Krzack, S.; Trimis, D.; Hasse, C.; Meyer, B. Development of an inverse diffusion partial oxidation flame and model burner contributing to the development of 3rd generation coal gasifiers. *Fuel Process. Technol.*, **2013**, *110*, 33-45.
[http://dx.doi.org/10.1016/j.fuproc.2013.01.005]
- [8] TU, Bergakademie Freiberg.; Meyer, B.; Gräbner, M.; Pardemann, R. Verfahren und Vorrichtung zur Flugstromvergasung fester Brennstoffe unter Druck. Patent *DE 10 2008 037 318 A1* 2010.
- [9] TU, Bergakademie Freiberg.; Meyer, B.; Seifert, P.; Krzack, S.; Ogriseck, S.; Rauchfuß, H.; Rieger, M.; Trompelt, M.; Guhl, S. Verfahren und Vorrichtung zur verschlackenden Vergasung fester Brennstoffe unter Druck. Patent *DE 10 2007 006 977 A1* 2008.
- [10] Gräbner, M.; Meyer, B. Introduction of a ternary diagram for comprehensive evaluation of gasification processes for ash-rich coal. *Fuel*, **2013**, *114*, 56-63.
[http://dx.doi.org/10.1016/j.fuel.2012.01.069]
- [11] Mason, D.M.; Patel, J.G. Chemistry of ash agglomeration in the U-Gas process. *Fuel Process. Technol.*, **1980**, *3*(3-4), 181-206.
[http://dx.doi.org/10.1016/0378-3820(80)90003-X]
- [12] Goyal, A.; Rehmat, A.; Knowlton, T.M.; Leppin, D.; Waibel, R.T.; Patel, J.G. Support studies for the U-GAS coal gasification process: Part I: Fluidization. *Fuel Process. Technol.*, **1987**, *17*(2), 169-186.
[http://dx.doi.org/10.1016/0378-3820(87)90076-2]
- [13] Goyal, A.; Rehmat, A.; Knowlton, T.M.; Leppin, D.; Waibel, R.T.; Patel, J.G. Support studies for the U-GAS coal gasification process: Part II: Combustion characteristics. *Fuel Process. Technol.*, **1988**, *17*(3), 209-219.
[http://dx.doi.org/10.1016/0378-3820(88)90036-7]
- [14] Zhang, Y. Biomass fluidized bed gasification for fuel gas. 2010. International Conference on IGCC & Xtl Technologies, 3.-5.5.2010, Dresden, Germany.
- [15] Haldipur, GB; Schmidt, DK; Smith, KJ A 50-month gasifier mechanistic study and downstream unit Process development program for the pressurized ash-agglomerating fluidized-bed gasification system *Final Report - Volume II*, **1988**.
- [16] Gräbner, M.; Meyer, B. Performance and exergy analysis of the current developments in coal gasification technology. *Fuel*, **2014**, *116*, 910-920.
[http://dx.doi.org/10.1016/j.fuel.2013.02.045]
- [17] Hsieh, C.R.; Roberts, P.T. A laboratory study of agglomeration in coal gasification; Preprints - American Chemical Society; Division of Petroleum Chemistry, 1985, Vol. 30.
- [18] Bartels, M.; Lin, W.G.; Nijenhuis, J. Agglomeration in fluidized beds at high temperatures: Mechanisms, detection and prevention. *Pror. Energy Combust. Sci.*, **2008**, *34*(5), 633-666.
[http://dx.doi.org/10.1016/j.pecs.2008.04.002]
- [19] Gupta, C.K.; Sathiyamoorthy, D. *Fluid bed technology in materials processing*; CRC Press: Boca Raton, Fla, **1999**.
- [20] Yang, W. *Handbook of fluidization and fluid-particle systems*; Marcel Dekker: New York, **2003**.
[http://dx.doi.org/10.1201/9780203912744]
- [21] Chen, D; Tang, L; Zhou, Y; Wang, W; Wu, Y; Zhu, Z Effect of char on the melting characteristics of coal ash. *J. fuel chem. and tech.*, **2007**, *35*(2), 136-40.
[http://dx.doi.org/10.1016/S1872-5813(07)60014-0]
- [22] Sandstrom, W.A.; Rehmat, A.G.; Bair, W.G. *A Fluidized-Bed Ash-Agglomeration Gasifier*, *Coal Processing Technology*, **1977**, *3*((A78-43403 13-44)), 180-186.

- [23] Nikrityik, P.; Meyer, B. *Gasification Processes – Modelling and Simulation*; Wiley-VCH: Weinheim, **2014**.
- [24] Adlhoch, W.; Keller, J.; Herbert, P.K. The development of the HTW coal gasification process. **1990.9th** conference, gasification power plants Palo Alto, California, USA
- [25] Laugwitz, A.; Gräbner, M.; Meyer, B. Modeling based development of internally circulating gasifier for high ash coals. Proceedings of the Pittsburgh Coal Conference Beijing, China 2013.
- [26] Schimpke, R.; Klinger, M.; Krzack, S.; Meyer, B. Determination of the initial ash sintering temperature by cold compression strength tests with regard to mineral transitions. *Fuel*, **2017**, *194*, 157-165.
[<http://dx.doi.org/10.1016/j.fuel.2016.12.066>]
- [27] Kunii, D.; Levenspiel, O. *Fluidization Engineering*; Butterworth-Heinemann: Stoneham, **1991**.
- [28] Duarte, C. R.; Murata, V. V.; Barrozo, M. A. S. A study of the fluid dynamics of the spouted bed using CFD. *Braz. J. Chem. Eng.*, **2005**, *22*(2) São Paulo
[<http://dx.doi.org/10.1590/S0104-66322005000200014>]
- [29] Reh, L. Das Wirbeln von körnigem Gut im schlanken Diffusor als Grenzzustand zwischen Wirbelschicht und pneumatischer Förderung., PhD-thesis: TH Karlsruhe, Germany, **1961**.

© 2017 Schurz *et al.*

This is an open access article distributed under the terms of the Creative Commons Attribution 4.0 International Public License (CC-BY 4.0), a copy of which is available at: <https://creativecommons.org/licenses/by/4.0/legalcode>. This license permits unrestricted use, distribution, and reproduction in any medium, provided the original author and source are credited.